Acta Crystallographica Section F
Structural Biology and Crystallization Communications
ISSN 1744-3091

The copper-containing amine oxidase from *Arthrobacter globiformis*: refinement at 1.55 and 2.20 Å resolution in two crystal forms

David B. Langley, Anthony P. Duff, Hans C. Freeman and J. Mitchell Guss*

School of Molecular and Microbial Biosciences, University of Sydney, NSW 2006, Australia

Correspondence e-mail: m.guss@mmb.usyd.edu.au

Received 21 August 2006
Accepted 22 September 2006

PDB References: AGAO, 1.55 Å resolution, 1w6g; 2.2 Å resolution, 1w6c.

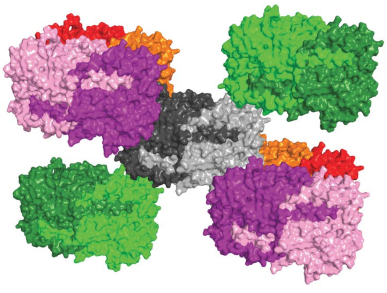

Copper-containing amine oxidases are found in all the major kingdoms of life. They catalyse the oxidation of organic amines in the presence of molecular dioxygen to aldehydes and hydrogen peroxide. The catalytic centres contain a Cu atom and a topaquinone cofactor formed autocatalytically from a tyrosine residue in the presence of Cu and molecular oxygen. The structure of the Cu-containing amine oxidase from *Arthrobacter globiformis*, which was previously refined at 1.8 Å resolution in space group *C*2 with unit-cell parameters $a = 157.84$, $b = 63.24$, $c = 91.98$ Å, $\beta = 112.0^\circ$ [Wilce *et al.* (1997), *Biochemistry*, **36**, 16116–16133], has been re-refined with newly recorded data at 1.55 Å resolution. The structure has also been solved and refined at 2.2 Å resolution in a new crystal form, space group *C*2, with unit-cell parameters $a = 158.04$, $b = 64.06$, $c = 69.69$ Å, $\beta = 111.7^\circ$.

1. Introduction

Copper-containing amine oxidases (CuAOs) contain a 2,4,5-trihydroxyphenylalanine quinone (TPQ) cofactor derived by a Cu-dependent self-processing post-translational oxidation of a conserved tyrosine residue (Cai & Klinman, 1994; Matsuzaki *et al.*, 1994; Wilce *et al.*, 1997). CuAOs, which catalyse the oxidative deamination of primary amines,

$$R\mathrm{CH_2NH_3^+} + \mathrm{O_2} + \mathrm{H_2O} \rightarrow R\mathrm{CHO} + \mathrm{NH_4^+} + \mathrm{H_2O_2},$$

have been found in a wide range of organisms, from bacteria to humans, and have been proposed to perform a variety of biological roles (Dove & Klinman, 2001). In microorganisms, amine oxidases generally have a nutritional role in the utilization of primary amines as the sole source of nitrogen or carbon. In plants, they have been implicated in wound healing. In mammals, functions such as detoxification have been identified and some CuAOs are known to be tissue-specific. In humans, an increased plasma concentration of a particular CuAO, vascular adhesion protein-1/semicarbazide-sensitive amine oxidase (VAP-1/SSAO), is known to be associated with metabolic and vascular diseases (Salmi & Jalkanen, 1996; Smith *et al.*, 1998).

Enzyme catalysis occurs in two half-reactions *via* a ping-pong mechanism (Dove & Klinman, 2001),

$$\mathrm{TPQ} + R\mathrm{CH_2NH_2} \rightarrow \mathrm{TPQ_{red}} + R\mathrm{CHO} \quad \text{(reductive half-reaction)},$$

$$\mathrm{TPQ_{red}} + \mathrm{O_2} + \mathrm{H_2O} \rightarrow \mathrm{TPQ} + \mathrm{NH_3} + \mathrm{H_2O_2} \quad \text{(oxidative half-reaction)}.$$

In the reductive half-reaction, the TPQ reacts with the amine substrate, releasing water and producing an intermediate substrate Schiff base. Several crystal structures of the molecule trapped in this state have been reported (O'Connell *et al.*, 2004; Wilmot *et al.*, 1997, 2004). A proton is abstracted, converting the substrate Schiff base to a product Schiff base. Hydrolysis yields a reduced aminoquinol ($\mathrm{TPQ_{red}}$) and the aldehyde product, which is released. In the oxidative half-reaction, two electrons are transferred from the aminoquinol to dioxygen. The mechanism of this electron transfer remains uncertain. Hydrogen peroxide is released and a final hydrolysis reaction frees ammonia and regenerates the TPQ cofactor.

CuAOs that have been characterized structurally include those from the bacteria *Escherichia coli* (ECAO; Parsons *et al.*, 1995) and *Arthrobacter globiformis* (AGAO; Wilce *et al.*, 1997), the plant *Pisum sativum* (PSAO; Kumar *et al.*, 1996), the yeasts *Hansenula polymorpha* (HPAO; Li *et al.*, 1998) and *Pichia pastoris* (Wilce *et al.*, 1997; Duff *et al.*, submitted) and two mammalian sources, bovine serum (BSAO; Lunelli *et al.*, 2005) and human plasma (VAP-1; Airenne *et al.*, 2005; Jakobsson *et al.*, 2005).

The CuAO from *A. globiformis* (AGAO) is one of the structurally best characterized enzymes of this class. Structures of AGAO that have been reported previously include the holoenzyme and apoenzyme (Wilce *et al.*, 1997), intermediates along the biogenetic pathway of the TPQ cofactor (Kim *et al.*, 2002) and complexes with inhibitors (O'Connell *et al.*, 2004). The molecule is a homodimer, in which each subunit has three domains. The N-terminal domains D2 and D3 pack against a large core consisting of the two symmetry-related D4 domains. Two long β-hairpin arms protrude from each D4 domain and embrace the other. A large solvent-filled cavity, described as a lake, lies between the two D4 domains. The cavity is connected to the external solvent *via* openings on and around the dimer twofold axis.

These properties, as well as the size and topology of the molecule, are shared with all other known CuAOs. ECAO alone has an additional N-terminal D1 domain in each subunit. Typically, one active site is buried deeply in each D4 domain and is accessed by substrates *via* a channel from the surface of the enzyme. The residues that line the channel belong to the D2, D3 and D4 domains of one subunit and to the tip of one of the β-hairpin arms of the symmetry-related subunit. Each active site contains a Cu^{II} atom and a TPQ cofactor. Three conserved histidine side chains coordinate the Cu. In the mature enzyme the TPQ has been observed in two conformations: an 'on-Cu' conformation, in which the O4 atom of TPQ is a Cu ligand, and an 'off-Cu' conformation, in which the Cu atom is not bonded to the TPQ and the reactive O5 atom of TPQ points into the substrate-binding site. In all native CuAO structures where the TPQ is off-Cu, a well ordered water molecule is observed in the position occupied by the O4 atom in the on-Cu structures. This position is usually described as 'axial'. In some CuAO structures, a water molecule is observed as a fifth Cu ligand in a position that is usually called 'equatorial'. In other structures no atom is modelled at this site, but a water molecule is modelled at 3.2–4.4 Å from the Cu. The Cu atom and its three histidine ligands are consistently well resolved, with Cu—N distances of ∼2.0 Å. In the previous structure of AGAO at room temperature, one of the histidine ligands, His592, was found in two conformations (Wilce *et al.*, 1997).

Four crystal forms of AGAO have been reported (Freeman *et al.*, 1996; Kim *et al.*, 2002). Structures have been published for only two of them, namely form II (PDB codes 1av4, 1avl and 1avk; Wilce *et al.*, 1997) and form IV [PDB codes 1ivx (Kim *et al.*, 2002) and 1iu7 (Kishishita *et al.*, 2003)]. The highest resolution achieved previously was 1.8 Å for form II. We now report the refinement of the structure of form II at 1.55 Å resolution, the first structure analysis of form I at 2.2 Å resolution and a comparison between the packings of the AGAO molecules in form I (space group *C*2), form II (space group *C*2) and form IV (space group *I*2).

2. Materials and methods

2.1. Enzyme purification and crystallization

AGAO was overexpressed recombinantly as a C-terminal StreptagII fusion. It was purified and concentrated using previously published protocols to a concentration of ∼10 mg ml^{-1} in 50 m*M* 4-(2-hydroxyethyl)-1-piperazineethanesulfonic acid (HEPES) buffer pH 7.0 (Juda *et al.*, 2001). Crystals were grown by vapour diffusion at 293 K in hanging drops containing 2 µl each of protein and well solution. The well solution for the form II crystals contained 1.6 *M* ammonium sulfate, 12%(*v*/*v*) dioxane and 100 m*M* morpholinoethanesulfonic acid (MES) pH 6.5 (Hampton Research Crystal Screen II condition No. 23). The well solution for the form I crystals contained 200 m*M* magnesium acetate, 20%(*m*/*v*) PEG 8000 and 100 m*M* sodium cacodylate pH 6.5. Large crystals, up to 500 × 400 × 100 µm in size, of the two crystal forms generally grew in two weeks.

2.2. Data collection and refinement

Prior to cryocooling, crystals were protected from freezing by the following protocol. Well solution was added to hanging drops containing the crystals to bring the total volume of the drop to 20 µl. The crystal drop was transferred to a sitting-drop well and the volume increased to 30 µl by the further addition of well solution. The drop solution was then progressively exchanged with well solutions containing 5%(*v*/*v*) increments of glycerol until the concentration of glycerol reached ∼30%(*v*/*v*). Half of the drop solution was removed and replaced by a new solution at each exchange. This process was repeated 12 times during 2 h with an increase in glycerol concentration at every second exchange. The crystals were cryocooled in a stream of cold N_2 gas at 100 K.

X-ray data were recorded at the Stanford Synchrotron Radiation Laboratory, beamline BL7-1 (λ = 1.08 Å), with a MAR Research 345 mm image-plate detector. Data were integrated using *DENZO* and scaled using *SCALEPACK* from the *HKL* suite of programs (Otwinowski & Minor, 1997). Refinement of the form II structure commenced with a model derived from the structure of AGAO previously refined at 2.2 Å resolution in the same unit cell (PDB code 1av4; Wilce *et al.*, 1997). All solvent molecules and metal ions were removed from the starting model and the TPQ cofactor (residue 382) was initially modelled as alanine. Initial calculations, including rigid-body, simulated-annealing and grouped *B*-factor refinement, were performed using *CNS* (Brünger *et al.*, 1998). The form I structure was solved by molecular replacement using *MOLREP* (Vagin & Teplyakov, 1997). The search model was the refined form II structure with all metal ions and solvent molecules removed and with the cofactor remodelled as alanine.

Following the initial model optimization, refinement protocols for both structures were the same and comprised cycles of refinement with *REFMAC*5 (Murshudov *et al.*, 1997), addition of water molecules with *ARP*/*wARP* (Perrakis *et al.*, 1999) and checking the model in electron-density maps ($F_{obs} - F_{calc}$ and $2F_{obs} - F_{calc}$). Water molecules and metal ions were added/deleted depending on their location in relation to significant electron density and the presence of satisfactory interactions for hydrogen bonding or coordination. Graphical manipulation of the models and inspection of electron-density maps were carried out with *O* (Jones *et al.*, 1991). The TPQ cofactors were only modelled in the final rounds of refinement. Structures were validated using *PROCHECK* (Laskowski *et al.*, 1993), *WHATCHECK* (Hooft *et al.*, 1996) and *MOLPROBITY* (Lovell *et al.*, 2003). The data-collection and refinement statistics are given in Tables 1 and 2.

3. Results and discussion

3.1. The structure of AGAO (form II) at 1.55 Å resolution

In the form II crystals, the asymmetric unit consists of one subunit, the AGAO dimer being generated by a crystallographic twofold axis.

Table 1
X-ray data statistics for AGAO.

Values in parentheses are for the highest resolution shell.

	Form II†	Form I†
Radiation wavelength (Å)	1.08	1.08
Space group	*C*2	*C*2
Unit-cell parameters		
a (Å)	157.84	158.04
b (Å)	63.24	64.06
c (Å)	91.98	69.69
β (°)	112.0	111.7
V (Å^3)	851272	655544
Subunits per ASU	1	1
Resolution range (Å)	25.8–1.55	28.3–2.20
Unique reflections	117993	31420
Completeness (%)	96 (87)	94 (85)
Redundancy	1.9 (1.8)	2.2 (2.0)
$\langle I/\sigma(I)\rangle$	10.8 (1.7)	13.8 (3.4)
$R_{\rm merge}$‡	0.04 (0.53)	0.05 (0.29)

† Three different forms of AGAO crystals were initially characterized (Freeman *et al.*, 1996). ‡ $R_{\rm merge} = \sum_h \sum_i |I_i - \langle I\rangle| / \sum_h \sum_i I_i$.

Table 2
Refinement statistics for AGAO.

Values in parentheses are for the highest resolution shell.

	Form II	Form I
No. of reflections used in refinement for $R_{\rm cryst}$	112062	29876
No. of reflections for $R_{\rm free}$	5927 (394)	1544 (110)
Composition of the final model		
Protein residues	620	620
Protein atoms	4868	4860
Residues with alternate conformers	10	0
Solvent atoms	506	144
Metal ions	2 Cu, 1 Na	2 Cu, 1 Na
Sulfate ions	2	0
Glycerol molecules	5	0
$\langle B\rangle$, protein atoms (Å^2)	12	27
$\langle B\rangle$, solvent atoms (Å^2)	45	31
$\langle B\rangle$, metal ions (Å^2)	33	29
$\langle B\rangle$, TPQ side chain (Å^2)	17 [0.3 occupancy]	34
$R_{\rm cryst}$†	0.171 (0.309)	0.183 (0.275)
$R_{\rm free}$‡	0.187 (0.309)	0.232 (0.310)
Ramachandran plot analysis§		
Allowed (%)	99.8	99.8
Favoured (%)	96.1	95.8
Outliers (%)	0.2	0.2
ESU based on maximum likelihood¶ (Å)	0.05	0.14
DPI†† (Å)	0.06	0.22
PDB code	1w6g	1w6c

† $R_{\rm cryst} = \sum_h |F_h({\rm obs}) - F_h({\rm calc})| / \sum_h F_h({\rm obs})$. ‡ $R_{\rm free} = R_{\rm cryst}$ for approximately 5% of the data not used during refinement. § Ramachandran plots were produced and analysed with *MOLPROBITY* (Lovell *et al.*, 2003). ¶ ESU, estimated standard uncertainty from the *REFMAC* refinement (Murshudov *et al.*, 1997). †† DPI, diffraction precision indicator (Cruickshank, 1999).

The model contains residues 9–628 of the polypeptide, two Cu atoms, one Na atom, two sulfate ions, five glycerol molecules (one of which is modelled in two conformations) and 506 water molecules. Ten residues are modelled with two side-chain conformations: Ser21, Ile39, Glu143, His201, Ile222, Ile351, Thr491, His592, Val596 and Met602. There is no significant electron density for the eight N-terminal and ten C-terminal residues or for the C-terminal Strep-tagII. A loop at residues 50–56 in the D2 domain is disordered. The atoms of these residues have relatively high displacement parameters. In the previously reported form II structure, the atoms of residues 50–56 were assigned zero occupancy (Wilce *et al.*, 1997).

The active-site Cu atom is coordinated by the N$^{\varepsilon2}$ atoms of His431 and His433, the N$^{\delta1}$ atom of His592 and by two water molecules (Table 3; Fig. 1*a*). The difference electron density for His592 was

Table 3
Copper geometry in AGAO.

	Form II†	Form I†	Form IV†
Cu–ligand distances (Å)			
His431	2.02	2.11	2.10
His433	2.06	2.06	2.16
His592	2.04 (2.18)‡	2.15	2.19
W_{ax}	2.25	§	2.03
W_{eq}	2.69 (2.16)¶	2.53	2.71
Angles at Cu (°)			
His431, His433	99	104	98
His431, His592	97	92	95
His431, W_{ax}	146	—	162
His431, W_{eq}	82	887	84
His433, His592	147	157	151
His433, W_{ax}	84	—	85
His433, W_{eq}	105	96	95
His592, W_{ax}	98	—	90
His592, W_{eq}	106	102	111
W_{ax}, W_{ax}	65	—	78

† Form II, AGAO refined at 1.55 Å resolution (PDB code 1w6g; this work). Form I, AGAO refined at 2.20 Å resolution (PDB code 1w6c; this work). Form IV, AGAO refined at 1.8 Å resolution (PDB code 1iu6; Kishishita *et al.*, 2003). ‡ The imidazole side chain of His592 is observed in two conformations. The distance to the minor conformer is given in parentheses. § No solvent molecule was modelled at the W_{ax} position in form I. ¶ The value in parentheses represents the Cu—O5(TPQ) distance. The TPQ was modelled in the 'on-Cu' conformation at 30% occupancy.

weak and it was modelled in two conformations related by a rotation of 66° about the C$^\alpha$—C$^\beta$ bond. The occupancies of the conformers were 0.8 and 0.2, respectively. The minor conformer of His592 has been reported previously in selected structures of AGAO (Kim *et al.*, 2002; Wilce *et al.*, 1997) but not in any other CuAO structure.

A feature shared with many CuAO native structures is the disorder of the TPQ cofactor (residue 382). Difference electron-density maps were consistent with ∼0.33 of the TPQ side chains being in the 'on-Cu' conformation, but were not sufficiently well resolved to model the ∼0.67 TPQ that is assumed to be in the 'off-Cu' conformation. Since the 'on-Cu' position of the TPQ quinone ring would clash with the axial and equatorial H_2O molecules coordinated to the Cu atom, these water molecules have been modelled with occupancies of 0.67 (Fig. 1*a*). The 'gate' residue, Tyr296, which opens a channel to the TPQ from the external solvent when inhibitors are bound (O'Connell *et al.*, 2004), is well ordered in its closed conformation.

Two additional metal-binding sites remote from the active site have been identified. An Na^+ ion near the protein surface is coordinated by Asp440 O$^{\delta1}$ (2.46 Å), Met441 O (2.48 Å), Asp581 O$^{\delta1}$ (2.58 Å), Ile582 O (2.49 Å) and a water molecule (2.80 Å) (Fig. 2*a*). The identification of this atom as an Na^+ ion was consistent with the heights of the relevant peaks in electron-density maps and with trigional-bipyramidal coordination geometry (Harding, 2006). An atom in the same location was identified as Mg^{2+} in the previous structure analysis of the form II crystals at lower resolution (Wilce *et al.*, 1997). A second Cu atom has been modelled on the protein surface, ∼20 Å from the active-site Cu atom (Fig. 2*b*). This second Cu atom was identified by its ligand geometry and by an anomalous scattering difference peak in a map produced from data recorded at the Cu absorption edge (data not shown). The ligand atoms are Asp161 O$^{\delta2}$ (2.32 Å), Asp165 O$^{\delta2}$ (2.28 Å), His170 N$^{\varepsilon2}$ (2.03 Å) and His201 N$^{\delta1}$ (1.94 Å). The side chain of the ligand His201 has two conformations. The minor conformer (occupancy 0.4) is coordinated to the Cu, which also has a refined occupancy of 0.4 (Fig. 2*b*).

3.2. The structure of AGAO (form I) at 2.2 Å resolution

The crystals of form I also contain one subunit molecule per asymmetric unit. The model consists of residues 9–628, 144 solvent

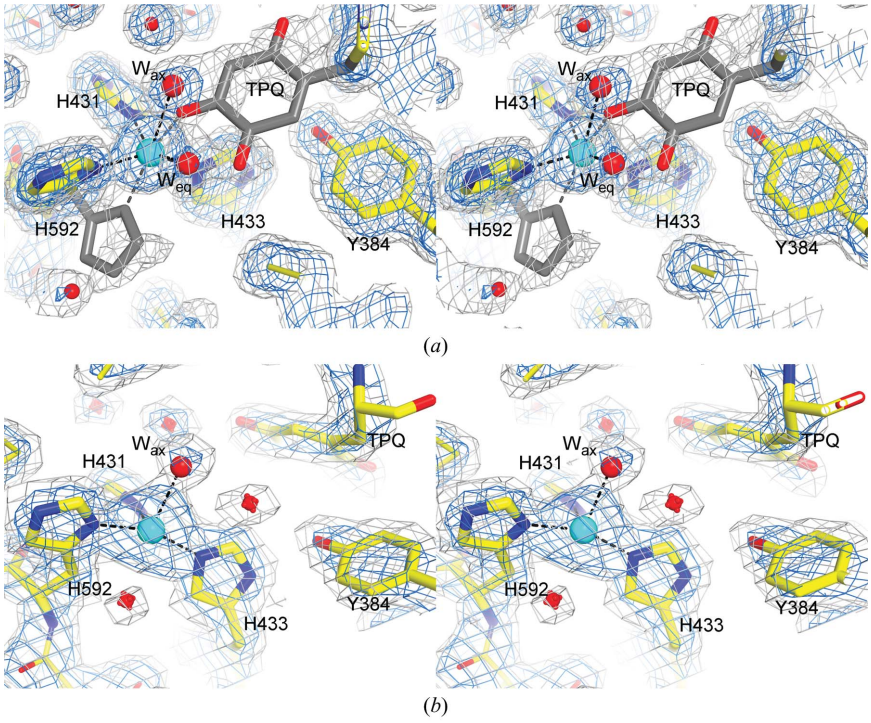

Figure 1
Stereoviews of the active site of AGAO. The Cu atoms and water molecules are shown as cyan and red spheres, respectively. (*a*) Cu site in the form II crystals. The second conformation of the Cu ligand, His592 and the C atoms of the disordered TPQ (occupancy 0.33) side chain are shown in grey. The 'axial' and 'equatorial' water ligands, W_{ax} and W_{eq}, to the Cu are displaced when the TPQ is in the shown 'on-Cu' conformation. The $2F_o - F_c$ electron density is contoured at 2σ (blue) and 0.7σ (grey). (*b*) Cu site in the form I crystals. Only the 'axial' water ligand, W_{ax}, was modelled. The TPQ is ordered in the 'off-Cu' conformation.

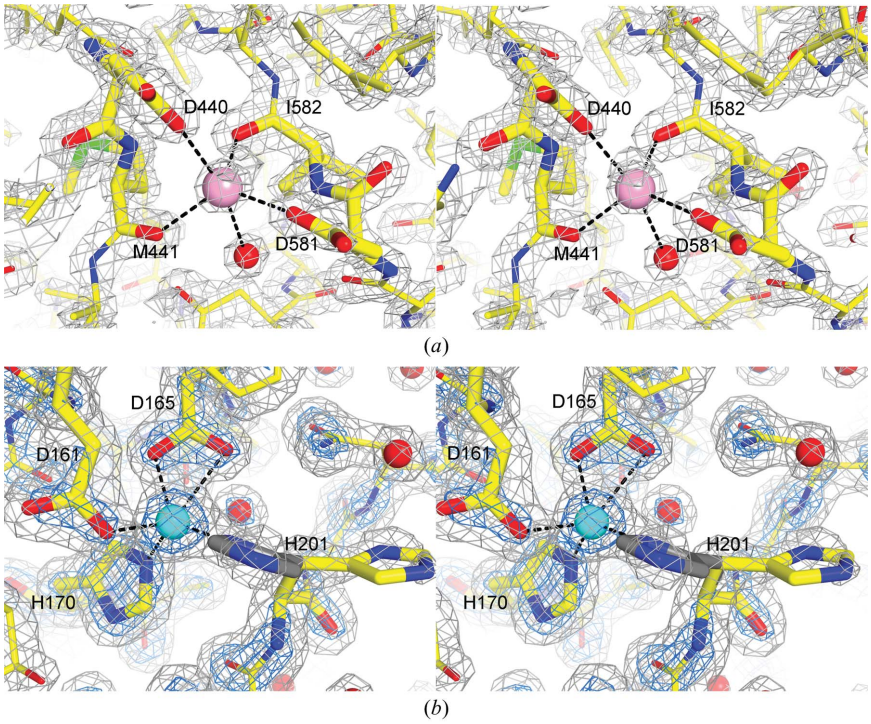

Figure 2
Stereoviews of the additional metal-binding sites in the form II crystals of AGAO. Water molecules are shown as red spheres. (*a*) The Na^+ ion (shown as a magenta sphere). This atom was modelled as Mg^{2+} in some other structures of AGAO. The $2F_o - F_c$ electron density is contoured at 1.5σ (grey). (*b*) The second Cu (shown as a cyan sphere). His592 adopts two conformations, one of which (shown with grey C atoms) is consistent with it acting as a ligand to the additional Cu atom. The second conformation of His592 (shown with yellow C atoms) is also adopted when the additional Cu atom is absent.

molecules, two Cu atoms and one Na^+ ion. The relatively lower resolution, 2.2 Å, precluded the modelling of alternate side-chain conformers, anions or glycerol molecules. For 620 C^α atoms observed in the polypeptide chains of both form I and form II, the r.m.s. difference is 0.27 Å. The maximum difference, 1.4 Å, occurs at residue 53, which is at the centre of a loop with high displacement parameters in both structures, consistent with disorder or flexibility. Thus, the subunit structure in form I is not significantly different from that in form II, but there are differences in structural details at the active site. Although the active-site Cu atom in form I is bound to the same three His residues as in form II, there is no evidence that the side chain of the ligand His592 has a second conformer (Fig. 1*b*). Furthermore, only the axial ligand H_2O molecule could be modelled in form I, since the difference electron density at the site of the equatorial H_2O molecule was very weak. The failure to model the second ligand water molecule and to observe the minor conformer of His592 may be a result of the lower resolution of this structure analysis. The TPQ is well ordered in the 'off-Cu' conformation and is modelled with full occupancy. The side chain of the 'gate' residue, Tyr296, is not associated with significant electron density. The implied disorder of this residue is surprising; in all other CuAO structures where the TPQ cofactor is ordered and in the 'off-Cu' conformation, the Tyr296 'gate' has been found to be ordered and 'open', so that substrates or inhibitors have access to the TPQ. The additional Cu^{2+} and Na^+ ions observed in form II are also observed in the structure of form I. The Cu atom at the remote site is assigned occupancy 0.3, although the electron density associated with the disordered His ligand of this Cu atom was too weak to model.

3.3. Intermolecular contacts in the four crystal forms of AGAO

Refined structures are now available for three of the four known crystal forms of AGAO (forms I, II and IV). The packing of the molecules in forms II and IV is essentially identical, except that the twofold symmetry relating the two halves of each dimer in form II is broken in form IV, resulting in a doubling of the volume of the asymmetric unit and the number of subunits contained within it. More importantly, the molecules in the form I cell are more tightly packed than those in forms II and IV. This is shown quantitatively by the Matthews coefficients (form I, 2.32 $Å^3\ Da^{-1}$; forms II and IV, 3.01 $Å^3\ Da^{-1}$) and by the solvent contents (form I, 46.6%; forms II and IV, 58.9%).

Consistent with the tighter packing in the crystals of form I, each subunit makes six crystal contacts with other dimers, compared with three

such contacts in forms II and IV (Fig. 3). In form I crystals, the four crystal contacts at the ends of each subunit are arranged in reciprocal pairs. The first pair of contacts involves residues 562–574 (helix) and 90–95 (loop) of one subunit and residues 16–29 (helix) and 79–83 (loop) of a subunit in a neighbouring dimer (Fig. 3*b*; contacts between either of the central grey subunits and the orange/red or pink/purple dimers). The second pair of contacts involves residues 117 (helix) and 187–189 (strand) of one subunit interacting with residues 163–164 (loop) of a neighbouring dimer (Fig. 3*b*; contacts between either of the grey subunits and the yellow/wheat or cyan/blue dimers). There is a further pair of contacts across crystallographic twofold axes. These involve residues 501–507 (loop) on each subunit to the same residues on a neighbouring dimer (Fig. 3*b*; contacts between either of the grey subunits and the pale pink/pale blue dimers).

In forms II and IV, the first pair of reciprocal contacts described for the form I crystals are preserved (Fig. 3; contacts from the grey subunits to the orange/red and pink/purple dimers). The third contact formed by each submit involves residues 123–126 (helix) and 196–197 (strand) of one subunit with a dimer related by a crystallographic twofold axis (Fig. 3*a*; contact between either of the grey subunits and the green/pale green dimer).

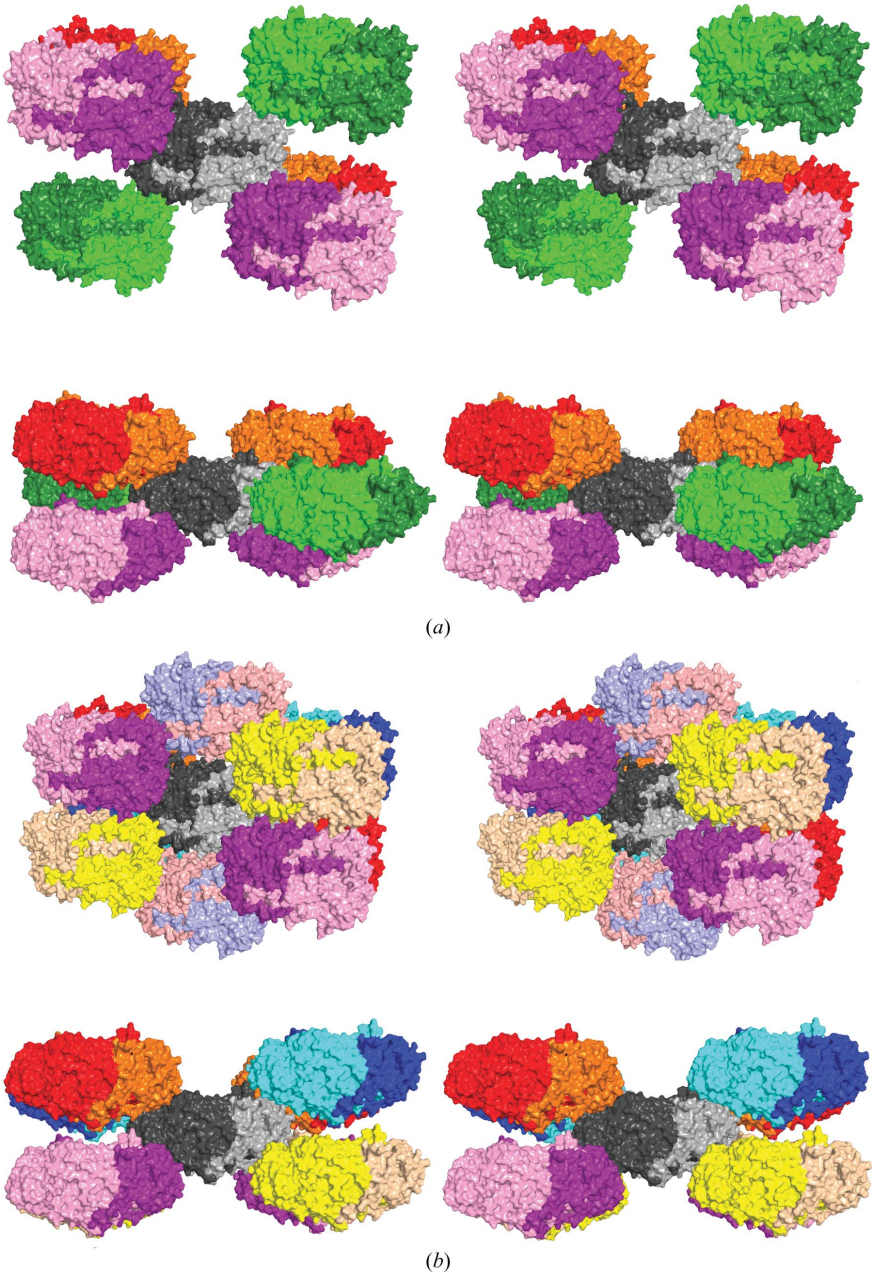

Figure 3
Unit-cell packing in the various crystal forms of AGAO. The top and bottom views in each panel are related by a 90° rotation about the *x* axis. (*a*) Forms II and IV. Each subunit is shown in a different colour or shade. Each subunit of the central dimer (grey or black) interacts directly with three other dimers (orange/red, green/light green and pink/purple). The packing in forms II and IV is nearly identical, but the crystallographic twofold axis relating the subunits of the dimer in form II is replaced by a local twofold axis in form IV. (*b*) Form I. Each subunit of the central dimer (grey or black) interacts directly with four dimers at each end (orange/red, blue/cyan, pink/purple and yellow/wheat) and two dimers near the centre (pale pink/pale blue). The central pair (pale pink/pale blue) has been omitted from the lower panel to reveal the central dimer.

3.4. Some comparisons with AGAO molecules in other crystal structures

The refinement of the AGAO structure in crystals of form II at 1.55 Å resolution has revealed new details but no significant differences from the previously published structures of forms II and IV at lower resolution (Kim *et al.*, 2002; Kishishita *et al.*, 2003; Wilce *et al.*, 1997). Multiple conformers are seen at ten residues and two additional metal-binding sites have been identified. Small segments of the polypeptide chain are disordered regardless of the resolution of the data, indicating that the disorder is a characteristic of the molecule. The TPQ side chain is poorly ordered with only 33% 'on-Cu', while the 'gate' residue Tyr296 is well ordered and 'closed'. This is in contrast with the active site in form I, where the TPQ is resolved, well ordered and 'off-Cu', while the side chain of the 'gate', Tyr296, is unresolved and disordered.

As indicated in §3.1 (above), one of the active-site Cu ligands, His592, is observed in two conformations in form II. The minor conformer has an occupancy of only 0.2. Of the 30 structures of native and inhibitor-complexed AGAO that have been refined in our laboratory, only form II at 1.55 Å resolution (present work) and the apoenzyme and holoenzyme at ambient temperature (Wilce *et al.*, 1997) have the side chain of His592 in two orientations. In a study of the conversion of Tyr382 to TPQ *via* freeze-trapped intermediates, the relationship between the occupancies of the two His592 conformers varied between 0:100 and 100:0 and the displacement parameters of the Cu atom appeared to be anisotropic (Kim *et al.*, 2002). The presence of two His592 conformers may be a symptom of incomplete occupancy of the Cu site. The additional metal site originally reported as an Mg^{2+} ion (Wilce *et al.*, 1997) has been modelled in the structures of form I and form II as Na^{+}. The nature of the metal ion was consistent with the arrangement of the ligands and the metal–ligand distances (Fig. 2*a*). Mg^{2+} would normally be expected to have a regular octahedral geometry

and shorter metal–ligand distances than observed in these structures (Harding, 2006). We note that although Wilce *et al.* (1997) reported the presence of an Mg^{2+} ion, the original PDB entries 1av4 and 1avl contain a water molecule at this position. In all other AGAO structures examined in the PDB, the atom now identified as a metal is modelled as a water molecule, despite the fact that this implies the presence of some improbably short hydrogen bonds.

Binding a second Cu^{2+} ion at the molecular surface of AGAO results in a change of the orientation of the side chain of one its ligands, His201. In structures of AGAO where this surface Cu is absent, a water molecule located ∼1 Å from the Cu position forms hydrogen bonds with the Cu ligands (Asp165, Asp161 and His170) and another solvent molecule. The second Cu site, which is observed in both forms I and II in the present work, has been reported in only one other AGAO structure (PDB code 1ui7). In that structure, a His433Ala mutation resulted in the absence of the Cu atom that normally occurs at the active site (Matsunami *et al.*, 2004). The cited authors concluded that the Cu atom at the second site originated from the additional $CuSO_4$ to which the protein had been exposed (Matsunami *et al.*, 2004). However, experiments on complexes of AGAO with benzyl hydrazine or tranylcypromine have shown that the addition of a similar excess of $CuSO_4$ to protein samples prior to crystallization does not necessarily lead to occupation of the second Cu site (Langley *et al*., 2006). It is possible that the affinity of this site for Cu depends not only on the Cu concentration in the buffer, but also on small changes of pH or other variables that are difficult to control in a crystallization drop. Since the second Cu site is ∼20 Å from the active-site Cu, it is unlikely to be of biochemical or physiological importance.

The work was supported by the Australian Research Council (DP0557353 to JMG and HCF). Portions of this research were carried out at the Stanford Synchrotron Radiation Laboratory, a national user facility operated by Stanford University on behalf of the US Department of Energy, Office of Basic Energy Sciences. Travel to SSRL was funded by the Access to Major National Facilities Programme administered by the Australian Nuclear Science and Technology Organization.

References

Airenne, T. T., Nymalm, Y., Kidron, H., Smith, D. J., Pihlavisto, M., Salmi, M., Jalkanen, S., Johnson, M. S. & Salminen, T. A. (2005). *Protein Sci.* **14**, 1964–1974.

Brünger, A. T., Adams, P. D., Clore, G. M., DeLano, W. L., Gros, P., Grosse-Kunstleve, R. W., Jiang, J.-S., Kuszewski, J., Nilges, M., Pannu, N. S., Read, R. J., Rice, L. M., Simonson, T. & Warren, G. L. (1998). *Acta Cryst.* D**54**, 905–921.

Cai, D. & Klinman, J. P. (1994). *J. Biol. Chem.* **269**, 32039–32042.

Cruickshank, D. W. J. (1999). *Acta Cryst.* D**55**, 583–601.

Dove, J. E. & Klinman, J. P. (2001). *Adv. Protein Chem.* **58**, 141–174.

Freeman, H. C., Guss, J. M., Kumar, V., McIntire, W. S. & Zubak, V. M. (1996). *Acta Cryst.* D**52**, 197–198.

Harding, M. M. (2006). *Acta Cryst.* D**62**, 678–682.

Hooft, R. W. W., Vriend, G., Sander, C. & Abola, E. E. (1996). *Nature (London)*, **381**, 272.

Jakobsson, E., Nilsson, J., Kallstrom, U., Ogg, D. & Kleywegt, G. J. (2005). *Acta Cryst.* F**61**, 274–278.

Jones, T. A., Zou, J.-Y., Cowan, S. W. & Kjeldgaard, M. (1991). *Acta Cryst.* A**47**, 110–119.

Juda, G. A., Bollinger, J. A. & Dooley, D. M. (2001). *Protein Expr. Purif.* **22**, 455–461.

Kim, M., Okajima, T., Kishishita, S., Yoshimura, M., Kawamori, A., Tanizawa, K. & Yamaguchi, H. (2002). *Nature Struct. Biol.* **9**, 591–596.

Kishishita, S., Okajima, T., Kim, M., Yamaguchi, H., Hirota, S., Suzuki, S., Kuroda, S., Tanizawa, K. & Mure, M. (2003). *J. Am. Chem. Soc.* **125**, 1041.

Kumar, V., Dooley, D. M., Freeman, H. C., Guss, J. M., Harvey, I., McGuirl, M. A., Wilce, M. C. J. & Zubak, V. M. (1996). *Structure*, **4**, 943–955.

Langley, D. B., Trambaiolo, D. M., Duff, A. P., Dooley, D. M., Freeman, H. C. & Guss, J. M. (2006). In preparation.

Laskowski, R. A., MacArthur, M. W., Moss, D. S. & Thornton, J. M. (1993). *J. Appl. Cryst.* **26**, 283–291.

Li, R., Klinman, J. P. & Mathews, F. S. (1998). *Structure*, **6**, 293–307.

Lovell, S. C., Davis, I. W., Arendall, W. B. III, de Bakker, P. I., Word, J. M., Prisant, M. G., Richardson, J. S. & Richardson, D. C. (2003). *Proteins*, **50**, 437–450.

Lunelli, M., Di Paolo, M. L., Biadene, M., Calderone, V., Battistutta, R., Scarpa, M., Rigo, A. & Zanotti, G. (2005). *J. Mol. Biol.* **346**, 991–1004.

Matsunami, H., Okajima, T., Hirota, S., Yamaguchi, H., Hori, H., Kuroda, S. & Tanizawa, K. (2004). *Biochemistry*, **43**, 2178–2187.

Matsuzaki, R., Fukui, T., Sato, H., Ozaki, Y. & Tanizawa, K. (1994). *FEBS Lett.* **351**, 360–364.

Murshudov, G. N., Vagin, A. A. & Dodson, E. J. (1997). *Acta Cryst.* D**53**, 240–255.

O'Connell, K. M., Langley, D. B., Shepard, E. M., Duff, A. P., Jeon, H. B., Sun, G., Freeman, H. C., Guss, J. M., Sayre, L. M. & Dooley, D. M. (2004). *Biochemistry*, **43**, 10965–10978.

Otwinowski, Z. & Minor, W. (1997). *Methods Enzymol.* **276**, 307–326.

Parsons, M. R., Convery, M. A., Wilmot, C. M., Yadav, K. D., Blakeley, V., Corner, A. S., Phillips, S. E., McPherson, M. J. & Knowles, P. F. (1995). *Structure*, **3**, 1171–1184.

Perrakis, A., Morris, R. & Lamzin, V. S. (1999). *Nature Struct. Biol.* **6**, 458–463.

Salmi, M. & Jalkanen, S. (1996). *J. Exp. Med.* **183**, 569–579.

Smith, D. J., Salmi, M., Bono, P., Hellman, J., Leu, T. & Jalkanen, S. (1998). *J. Exp. Med.* **188**, 17–27.

Vagin, A. A. & Teplyakov, A. (1997). *J. Appl. Cryst.* **30**, 1022–1025.

Wilce, M. C. J., Dooley, D. M., Freeman, H. C., Guss, J. M., Matsunami, H., McIntire, W. S., Ruggiero, C. E., Tanizawa, K. & Yamaguchi, H. (1997). *Biochemistry*, **36**, 16116–16133.

Wilmot, C. M., Murray, J. M., Alton, G., Parsons, M. R., Convery, M. A., Blakeley, V., Corner, A. S., Palcic, M. M., Knowles, P. F., McPherson, M. J. & Phillips, S. E. (1997). *Biochemistry*, **36**, 1608–1620.

Wilmot, C. M., Saysell, C. G., Blessington, A., Conn, D. A., Kurtis, C. R., McPherson, M. J., Knowles, P. F. & Phillips, S. E. (2004). *FEBS Lett.* **576**, 301–305.